RSC Advances

Multiferroic properties of Bi0.5K0.5TiO3-BiFe1−xCoxO3 (0 ≤ x ≤ 0.2) solid solution

Journal:	*RSC Advances*
Manuscript ID	RA-ART-09-2015-019768.R1
Article Type:	Paper
Date Submitted by the Author:	16-Nov-2015
Complete List of Authors:	Zuo, Xuzhong; Chinese Academy of Sciences, Institute of Solid State Physics Yang, Jie; Chinese Academy of Sciences, Institute of Solid State Physics Yuan, Bin; Chinese Academy of Sciences, Institute of Solid State Physics Kan, Xucai; Chinese Academy of Sciences, Institute of Solid State Physics Zu, Lin; Chinese Academy of Sciences, Institute of Solid State Physics Qin, Yanfeng; Chinese Academy of Sciences, Institute of Solid State Physics Zhu, Xuebin; Chinese Academy of Sciences, Institute of Solid State Physics Song, Wenhai; Chinese Academy of Sciences, Institute of Solid State Physics Sun, Yunping; Chinese Academy of Sciences, Institute of Solid State Physics
Subject area & keyword:	Electronic materials < Materials

RSC Advances
CREATED USING THE RSC LaTeX PCCP ARTICLE TEMPLATE – SEE www.rsc.org/electronicfiles FOR DETAILS
ARTICLE TYPE www. rsc.org/xxxxxx | XXXXXXXX

Multiferroic properties of $Bi_{0.5}K_{0.5}TiO_3$-$BiFe_{1-x}Co_xO_3$ ($0 \leq x \leq 0.2$) solid solution

X. Z. Zuo,[a] J. Yang,* [a] B. Yuan,[a] X. C. Kan,[a] Lin Zu,[a] Y. F. Qin,[a] X. B. Zhu,[a] W. H. Song,* [a] and Y. P. Sun,[abc]

DOI: 10.1039/b000000x

Fabrication of $BiFeO_3$ and $Bi_{0.5}K_{0.5}TiO_3$ typically meet problems with densification and phase purity, requiring high pressure conditions for synthesis of bulk phases. In this letter, we have successfully prepared a binary lead-free solid-solution of $Bi_{0.5}K_{0.5}TiO_3$-$BiFe_{1-x}Co_xO_3$ using a modified Pechini method and investigated the magnetic and ferroelectric properties of $Bi_{0.5}K_{0.5}TiO_3$-$BiFe_{1-x}Co_xO_3$ ($0 \leq x \leq 0.2$). The coexistence of room-temperature ferromagnetism and ferroelectricity is observed in $Bi_{0.5}K_{0.5}TiO_3$-$BiFe_{1-x}Co_xO_3$ ($0.5 \leq x \leq 0.2$). The x=0.2 sample exhibits ferromagnetic behavior with Curie temperature T_C of 661 K compared with the paramagnetic like behavior in $Bi_{0.5}K_{0.5}TiO_3$-$BiFeO_3$ at room temperature. The ferromagnetism can be ascribed to the suppression of spiral spin structure with the canting of the anti-ferromagnetically ordered spins caused by structural distortion due to the the substitution of Co ions. The x=0.2 sample also exhibits a well-defined ferroelectric hysteresis loop with a rather large remnant polarization (P_r = 32.72 $\mu C/cm^2$), which is superior to that of other lead-free ferroelectric compounds. The improved ferroelectric properties can be attributed to the increased grain size and lattice distortion caused by Co doping. The observation of room temperature ferromagnetism and ferroelctricity for $Bi_{0.5}K_{0.5}TiO_3$-$BiFe_{1-x}Co_xO_3$ suggests that these materials are potential candidates for multiferroic materials and ferroelectric memory.

1 Introduction

Recently, much attention has been paid to multiferroic materials which simultaneously exhibits the combination of ferroelectricity, ferromagnetism, and/or ferroelasticity. And also, the coupling effect of electrical and magnetic order parameters offer wide range of novel applications as magnetic sensors, transformers, multiple state memories and microwave devices.[1–4] Unfortunately, there are very less number of single phase materials that exhibit the coexistence of room temperature ferromagnetism and ferroelectricity reported in literatures. Among all the known multiferroics, $BiFeO_3$ (BFO) is one of the most promising materials for device applications due to its high FE Curie temperature ($T_C \sim 1103$ K) and antiferromagnetic (AFM) temperature ($T_N \sim 643$ K).[5,6] In BFO, the AFM spin structure is of G-type. This spatially modulated cycloidal spin structure does not allow the appearance of net magnetization and inhibits the observation of a notable linear ME effect in BFO.[7] Therefore, it is expected to get non-zero magnetization and linear ME effect in BFO by suppressing or destroying the spin cycloid, which can be realized via chemical substitution. Naganuma et al.[8] found that substitution of Co for Fe induces a ferromagnetic spontaneous magnetization at room temperature (RT). However, BFO and doped compounds generally have a high leakage current density at room temperature.[9] It is known that perovskite ceramic based on mixed bismuth and alkali A-cations $Bi_{0.5}K_{0.5}TiO_3$ (BKT) is one candidate of lead-free piezoelectric material with a large spontaneous polarization and high Curie temperature.[10–12] Unfortunately, BKT ceramic do not exhibit ferromagnetism at RT. We should also note that both BFO and BKT ceramic have been reported to be challenging to prepare by the conventional ceramic processes because the synthesis of bulk phases requires high pressure conditions.[9] Hence, it is natural to combine the advantages of Co doped BFO with ferromagnetic ordering and BKT with high remnant polarization to obtain a solid solution system that possess an enhanced magnetism and ferroelectricity. Moreover, previous studies mostly focused on the ferroelectric and piezoelectric properties of BKT-BFO solid solution. Until now, the magnetic properties of BKT-BFO and the Co-doped BKT-$BiFe_{1-x}Co_xO_3$ have not yet been revealed in literature.[14–16] In this letter, we systematically investigated the magnetic and ferroelectric properties of $Bi_{0.5}K_{0.5}TiO_3$-$BiFe_{1-x}Co_xO_3$ ($0 \leq x \leq 0.2$) by using the measurements of magnetization and ferroelectricity. We found that the Co-doped BKT-BFO samples present a remarkable coexistence of ferroelectricity and ferromagnetism at RT. The results indicate that it is an effective way to explore RT multiferroics compound through a binary solid-solution since RT multiferroics is extremely rare.[6,9,18,19]

[a] *Key Laboratory of Materials Physics, Institute of Solid State Physics, Chinese Academy of Sciences, Shushanhu Road 350, Hefei 230031, Peoples Republic of China. E-mail: jyang@issp.ac.cn, E-mail: whsong@issp.ac.cn*
[b] *High Magnetic Field Laboratory, Chinese Academy of Sciences, Hefei 230031, People's Republic of China.*
[c] *Collaborative Innovation Center of Advanced Microstructures, Nanjing University, Nanjing 210093, Peoples Republic of China.*

2 Experiment

It is well known that the ionic radius of Co^{3+} (0.61 Å) is slightly smaller than that of Fe^{3+} (0.645 Å). Therefore, the Co substitution of Fe in BKT-$BiFe_{1-x}Co_xO_3$ will result in lattice distortion and the lattice contraction. Hence, the realization of a high-level substitution becomes difficult. Fortunately, we have successfully synthesized BKT-$BiFe_{1-x}Co_xO_3$ polycrystalline samples with x as high as 0.2, whereas impurity phase can be detected when the doping level is beyond 0.2. BKT-$BiFe_{1-x}Co_xO_3$ ($0 \leq x \leq 0.2$) samples were synthesized with a modified Pechini method which maintains atomic-level mixing of metal cations so as to lower sintering temperature in the sake of minimization of the volatility of Bi and K. Stoichiometric amounts of the starting materials, , KNO_3, $Bi(NO_3)_3{\cdot}5H_2O$, $Fe(NO_3)_3{\cdot}9H_2O$, and $Co(CH_3COO)_2{\cdot}4H_2O$ were dissolved into the citric acid monohydrate $C_6H_8O_7{\cdot}H_2O$ solution with glycol and acetic acid in stoichiometric proportions. Citric acid monohydrate $C_6H_8O_7{\cdot}H_2O$ was added to the solution as a complexant. Glycol was used for adjusting the viscosity and stability of the sol. Ammonia was added into the mixture of these solutions to adjust pH to 7 and the mixture was stirred until transparent precursor sol was obtained. Then the precursor solution was heated on a hot plate at 90 °C resulting in the formation of a gel. The gel was heated at 400 °C to remove the organic species. The obtained powders were mixed and grounded, and then calcined at 700 °C for 10 h under an O_2 flow, then, the obtained powders were ground, pelletized, and sintered at 800 °C for 20 h under an O_2 flow with two intermediate grindings, and finally the furnace was cooled slowly to room temperature. The x-ray powder diffraction patterns were recorded at RT on a Panalytical diffractometer (XPert PROMRD) with Cu Kα radiation and a graphite monochromator in a reflection mode. Structural refinement of powder BKT-$BiFe_{1-x}Co_xO_3$ ($0 \leq x \leq 0.2$) (BKT-BFC) sample was carried out by using RIETICA software. The average stoichiometry of BKT-$BiFe_{1-x}Co_xO_3$ ($0 \leq x \leq 0.2$) polycrystalline was determined by examination of multiple points using an energy-dispersive x-ray spectroscopy (EDX) in a JEOL JSM-6500 scanning electron microscope. The microstructure was observed using a field emission scanning electron microscope (FESEM, Sirion 200, FEI Company). The temperature dependence of magnetization was carried out from 300 to 850K using a Physical Property Measurement System-vibrating sample magnetometer (PPMS-VSM) with a high-temperature oven option. The magnetization hysteresis measurements were performed with a Quantum Design superconducting quantum interface device (SQUID) magnetic property measurement system (MPMS) system ($2 \leq T \leq 400$ K, $0 \leq H \leq 5$ T). The ferroelectric properties were investigated using a Sawyer-Tower circuit attached to a computer-controlled standardized ferroelectric test system (Radiant Technology 609B) with probes on the electrodes of the samples, which were immersed in silicone oil to prevent arcing.

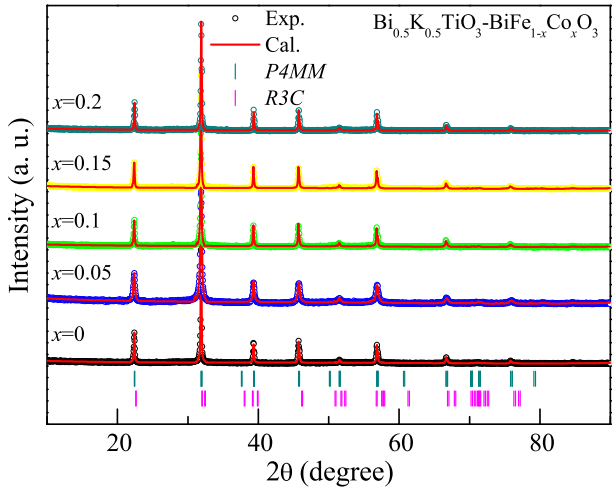

Fig. 1 (a) XRD patterns of $Bi_{0.5}K_{0.5}TiO_3$-$BiFe_{1-x}Co_xO_3$ ($0 \leq x \leq 0.2$). Circles indicate the experimental data, and the calculated data are the continuous line overlapping them. The vertical bars indicated the expected reflection positions for *P*4*mm* and *R*3*c* space group.

3 Results and Disscussion

Figure 1 shows the XRD patterns of BKT-$BiFe_{1-x}Co_xO_3$ ($0 \leq x \leq 0.2$) at room temperature. All the patterns can be indexed to a single phase with perovskite type structure. Previous researchers have reported that the refinement of the patterns using the space groups of the two end members ($Bi_{0.5}K_{0.5}TiO_3$ and $BiFeO_3$) or a cubic perovskite was challenging due to peak broadening and strain effects.[14] Therefore, we refined the samples to obtain the structural parameters and mole percentage with two-phase fitting ($Bi_{0.5}K_{0.5}TiO_3$ and $BiFe_{1-x}Co_xO_3$ with *P*4*mm* and *R*3*c* space group, respectively) by using the program Rietica. The experimental and calculated XRD patterns of BKT-$BiFe_{1-x}Co_xO_3$ are shown in Fig. **??**. The structural parameters obtained from the Rietveld refinements are listed in Tables 1. The fit between the experimental and calculated XRD patterns is relatively good based on the consideration of the lower R_P for all samples. The fractional atomic coordinates of BKT-$BiFe_{0.8}Co_{0.2}O_3$ determined by two-phase refinement of x-ray data are shown in table 2. Figure 2 shows the dependence of refined lattice parameters of BKT (*P*4*mm*) and $BiFe_{1-x}Co_xO_3$ (*R*3*c*) on the doping level of Co ions. The obtained lattice parameters are consistent with the previous reported results for BKT and $BiFeO_3$, respectively.[5,6] From Fig. 2, the following features are noted: (1) Increasing the doping level of Co does not change *a*, *b*, and *c* in BKT; (2) the slightly decrease in *a*, *b*, *c* and the volume of the

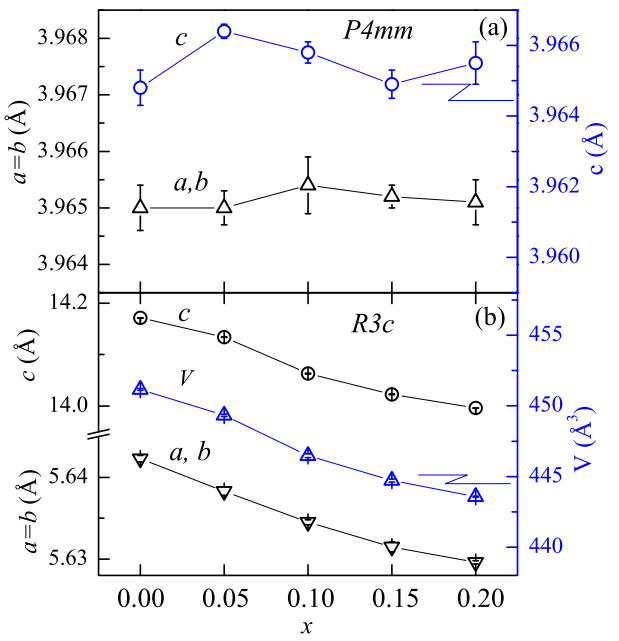

Fig. 2 (a) Lattice parameters a, b, and c, as a function of the doping level of Co for $Bi_{0.5}K_{0.5}TiO_3$ with $P4mm$ space group. (b) Lattice parameters a, b, c, and V, as a function of the doping level of Co for $BiFe_{1-x}Co_xO_3$ with $R3c$ space group.

unit cell V with increasing the content Co in $BiFe_{1-x}Co_xO_3$ can be found. The lattice shrinks upon Co doping can be attributed to the ionic radii of Co ions (0.61 Å) is smaller than that of the Fe ions (0.645 Å). Fig. 3(a)-(e) shows the representative scanning electron microscopy (SEM) images obtained from the surface of BKT-$BiFe_{1-x}Co_xO_3$ ceramics. It can be seen from Fig. 3 that the grain of all samples has the nearly quadrate feature and the grain size increases obviously upon increasing amount of Co, indicating the doping of Co ions can effectively promote the grains growth. The EDX analysis of the samples confirms the presence of K, Bi, Ti, Fe and Co, and the typical sample x=0.2 was given in Fig. 3(f). The average atomic ratios determined from EDX spectra are well consistent with the formula of BKT-$BiFe_{0.8}Co_{0.2}O_3$.

Table 1 Structural parameters of $Bi_{0.5}K_{0.5}TiO_3$-$BiFe_{1-x}Co_xO_3$ ($0 \leq x \leq 0.2$) obtained from Rietveld analysis at room temperature.

x	Space group	R_p	R_{wp}	χ^2	mol.%
0	P4mm/R3C	3.45	3.22	0.732	50.67/49.33
0.05	P4mm/R3C	4.12	3.73	0.659	49.8/50.2
0.1	P4mm/R3C	4.21	3.94	0.951	49.86/50.14
0.15	P4mm/R3C	4.48	4.11	0.866	50.21/49.79
0.2	P4mm/R3C	4.67	4.36	1.042	49.93/50.07

Figure 4 shows the field dependence of magnetization of BKT-$BiFe_{1-x}Co_xO_3$ (BKT-BFCO) samples at RT. For the Co-

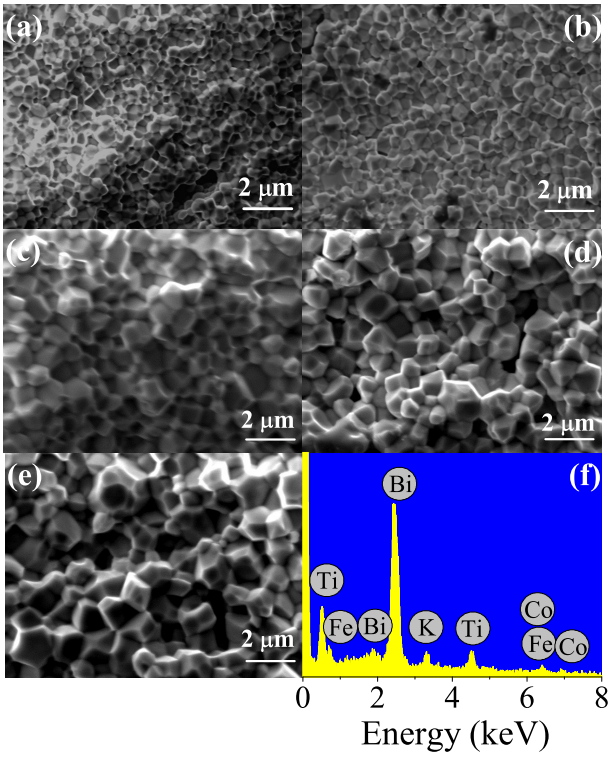

Fig. 3 Representative SEM images of $Bi_{0.5}K_{0.5}TiO_3$-$BiFe_{1-x}Co_xO_3$ with (a) x = 0,(b) x = 0.05, (c) x = 0.1, (d) x = 0.15, (e) x = 0.2. (f) The EDX spectrum of $Bi_{0.5}K_{0.5}TiO_3$-$BiFe_{0.8}Co_{0.2}O_3$ sample.

free sample, the M-H plot exhibits a linear behavior implying the characteristics of paramagnetic (PM) and/or antiferromagnetic (AFM). The temperature dependence of magnetization of the Co-free sample in the zero-field cooled (ZFC) and field cooled (FC) modes in a magnetic field of 100 Oe from 5 to 300K was measured. The superposition of the FC and ZFC magnetization manifests BKT-BFO is a PM like intraction (do not shown here). Upon Co doping, the M-H plots of BKT-BFCO samples gradually exhibit a hysteresis loop behavior. A large hysteresis loop of the x=0.2 sample can be observed (right inset of Fig. 4) with a remnant magnetization M_r of 0.15 emu/g and coercive field H_c of 734 Oe. In addition, the magnetization do not reach saturation up to H=4.5T implying the coexistence of FM and AFM interactions in BKT-BFCO samples. A liner extrapolation of M(H) to H=0 allows us to determine the spontaneous magnetization Ms of x=0.2 sample as 0.065 μ_B/f.u. This value is much smaller than the mean spin only value of isolated Fe^{3+} (2.5μ_B), and Co^{3+} (2μ_B) ions implying that the FM did not originate from the Fe or Co clusters but from the interactions between Fe^{3+} and Co^{3+} via the medium of oxygen. To make clear the nature of BKT-$BiFe_{0.8}Co_{0.2}O_3$ sample, we measured the temperature depen-

Table 2 Fractional atomic coordinates of $Bi_{0.5}K_{0.5}TiO_3$-$BiFe_{0.8}Co_{0.2}O_3$ determined by two-phase refinement of x-ray data.

Atom	*x*	*y*	*z*	occupancy
$Bi_{0.5}K_{0.5}TiO_3$				
Bi	0	0	-0.0453(3)	1/16
K	0	0	-0.0453(3)	1/16
Ti	0.5	0.5	0.5	1/8
O1	0.5	0.5	0.0021(5)	1/8
O2	0.5	0	0.5269(1)	1/4
$BiFeO_3$				
Bi	0	0	0	1/3
Fe	0	0	0.2208(3)	1/3
O	0.4421(4)	0.0187(1)	0.9522(6)	1

dence of magnetization for BKT-$BiFe_{0.8}Co_{0.2}O_3$ in an applied field of 100 Oe, as shown in Figure 5. It is found that there is a deviation between the ZFC magnetization (M_{ZFC}) and the FC magnetization (M_{FC}) curves below 652 K. The sample seems to undergo a PM-to-FM magnetic transition at 659.5 K (defined as the temperature corresponding to the dip of dM/dT, as shown in the inset of Fig. 5. Moreover, the M_{ZFC} exhibits a cusp at the temperature of 630 K. The experimental features regarding the typical irreversibility found in M_{FC} and M_{ZFC} with a cusp in the plot of M_{ZFC} as well as the non-saturation of the FC magnetization at temperatures far below T_C are reminiscent of cluster glasses. The temperature dependence of inverse magnetic susceptibility χ_m ($1/\chi_m$ =H/M) of BKT-$BiFe_{0.8}Co_{0.2}O_3$ is shown in right panel of Fig. 5. For a ferromagnet in the PM region, the relation between χ_m and temperature T should follow the Curie-Weiss law, i.e., $\chi_m = C_m/(T - \theta_p)$, where C_m is the molar Curie constant, and θ_p is the paramagnetic Curie temperature. The solid line is the calculated curve deduced from the Curie-Weiss equation. It is found that the experimental curve in the whole PM temperature range can be well described by the Curie-Weiss law. The paramagnetic Curie temperature θ_p can be determined to be 660.7 $\pm$ 1.4 K, which almost coincides with the value of T_C. For BKT-$BiFe_{0.8}Co_{0.2}O_3$, the effective magnetic moment deduced from the Curie constant C_m can be determined to be μ_{eff} = 4.88 $\pm$ 0.37 μ_B. In a mean field approximation, for one type of magnetic ions, the expected paramagnetic effective moment μ_{eff} is given by $\mu_{eff}^2 = xg^2S(S+1)\mu_B^2$, where x is the fraction of magnetic ions per formula unit, g the gyromagnetic factor, and S their spin quantum number. As a result, the expected effective moment μ_{eff} of BKT-$BiFe_{0.8}Co_{0.2}O_3$ can be obtained as μ_{eff} =5.72 μ_B. It can be seen that the expected effective moment (5.72 μ_B) is in agreement with the experimental data (4.88 $\pm$ 0.37 μ_B) implying that both Fe^{3+} and Co^{3+} contribute to the magnetization of BKT-$BiFe_{0.8}Co_{0.2}O_3$. The appearance of ferromagnetism in solid solution systems can be attributed to different magnetic moment of Co^{3+} and Fe^{3+}, which suppresses or breaks the spiral spin structure, as reported by others[8,20], or the canting of the anti-ferromagnetically ordered spins due to structural distortion.[21,22]

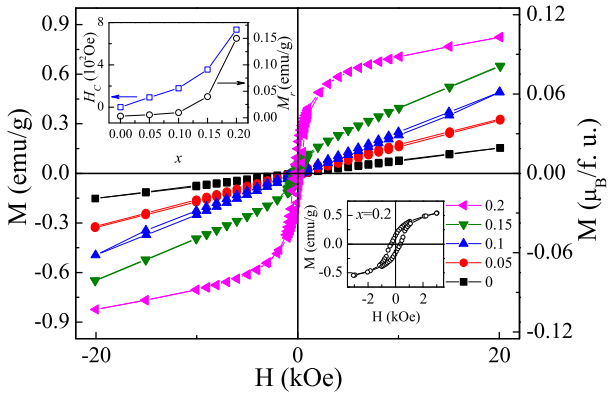

Fig. 4 Room temperature M-H hysteresis loops of $Bi_{0.5}K_{0.5}TiO_3$-$BiFe_{1-x}Co_xO_3$ samples. The left inset shows M_r and H_c vs. the doping level of Co. The right inset denotes the enlarged part of magnetic hysteresis of the x=0.2 sample in the low field.

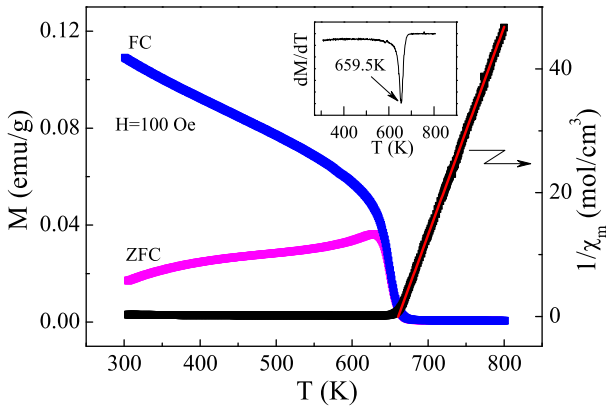

Fig. 5 Temperature dependence of magnetization and reverse magnetic susceptibilities for $Bi_{0.5}K_{0.5}TiO_3$-$BiFe_{0.8}Co_{0.2}O_3$ in the ZFC and FC modes measured at H=100 Oe. The solid lines are the best fits to the Curie-Weiss law and the inset are the plot of dM/dT.

The polarization-electric field (P-E) hysteresis of BKT-BFCO samples measured at RT under the applied electric field 100 kV/cm and the applied frequency of 100 Hz is shown in Fig. 5. P-E hysteresis loops of all the BKT-BFCO samples show a superior ferroelectric property. The inset shows the evolution in the P_r and E_c values as a function of the Co-doping level for BKT-BFCO samples. It can be seen that both the P_r and E_c increases monotonically with increasing the doping level of Co, and the remnant polarization has the maximum value P_r= 32.72 μC/cm^2

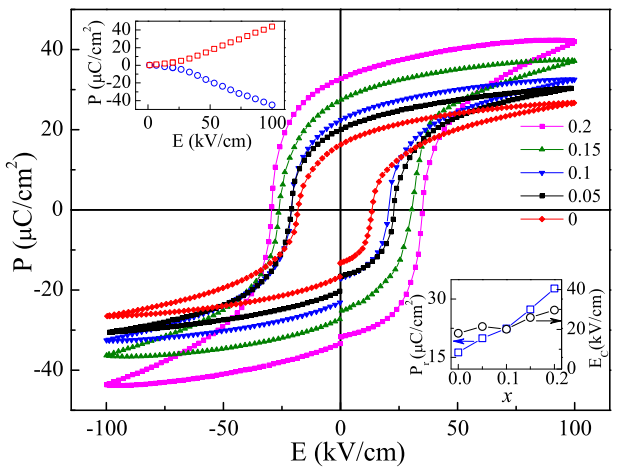

Fig. 6 RT ferroelectric hysteresis loop of $Bi_{0.5}K_{0.5}TiO_3$-$BiFe_{1-x}Co_xO_3$ samples measured under an electrical field of 100 kV/cm. The left inset shows plot of switched polarization vs pulse amplitude for $Bi_{0.5}K_{0.5}TiO_3$-$BiFe_{0.8}Co_{0.2}O_3$ from a PUND measurement. The right inset denotes P_r and E_c vs. the doping level of Co.

for the x=0.2 sample. This value is larger than that of $(Bi_{0.5}Na_{0.5})TiO_3$-$BiFeO_3$(31 $\mu C/cm^2$),[23] $Bi(Zn_{0.5}Ti_{0.5})O_3$-$(Bi_{0.5}K_{0.5})TiO_3$-$(Bi_{0.5}Na_{0.5})TiO_3$ (17 $\mu C/cm^2$),[24] and 1-x-y$(Bi_{0.5}Na_{0.5}TiO_3)$-x$Bi_{0.5}K_{0.5}TiO_3$-y$K_{0.5}Na_{0.5}NbO_3$ (28 $\mu C/cm^2$)[25] prepared by a solid state synthesis, which have been extensively investigated as candidates for the lead-free ferroelectrics. Considering that we prepared the sample with a sol-gel method and sintered at 800 °C for 20 h under an O_2 flow. It is suggested that ferroelectric materials prepared under oxygen atmosphere and low temperature will suppress the formation of oxygen vacancies and volatilization of Bi in processing, respectively, which will give rise to the increased ferroelectric polarization compare to the ferroelectric material prepared by solid state reaction.[26] To rule out a possibility of artificial polarization from leakage, we performed the pulsed polarization positive-up-negative-down (PUND) measurement and the results are shown in inset of Fig. 6. The measured switched polarization value is close to $2P_r$ obtained from the P-E loops implying that we can rule out the contribution of the leakage current to the remnant polarization. From Fig. 6, one can also see that the ferroelectric polarization of the samples increases with the increase in the Co-doping level. From Fig. 2, it can be seen that the grain size increases with the increase in the Co-doping level. The increased grain size will result in the increase in the remnant polarization.[27] Previous results have demonstrated that the lattice distortion can also affect the ferroelectric polarization of the displacement ferroelectrics because of the crystal anisotropy of the ferroelectric phase in perovskite ferroelectrics such as $Bi_6Ti_3Fe_2O_{18}$, $BiFeO_3$, $PbTiO_3$ and $BaTiO_3$.[28–30] Therefore, the enhancement of ferroelectric polarization in BKT-BFCO samples can be attributed to the combination of the lattice distortion and the increased grain size caused by Co doping.

4 Conclusions

In summary, we have studied the structural, magnetic, and ferroelectric properties of $Bi_{0.5}K_{0.5}TiO_3$-$BiFe_{1-x}Co_xO_3$ ($0 \leq x \leq 0.2$) solid solution. The Co-doped $Bi_{0.5}K_{0.5}TiO_3$-$BiFeO_3$ samples exhibit FM behavior at RT. The FM property in $Bi_{0.5}K_{0.5}TiO_3$-$BiFe_{1-x}Co_xO_3$ sample is proposed to originate from the suppression of spiral spin structure with the canting of the anti-ferromagnetically ordered spins caused by structural distortion due to the the substitution of Co ions. Both the P_r and E_c increase monotonically with increasing the doping level of Co and the x=0.2 sample shows the largest remanent polarization P_r of 32.72$\mu C/cm^2$, and the improved ferroelectric property can be attributed to the combination of the increased grain size and lattice distortion.

Acknowledgments

This work was supported by the National Natural Science Foundation of China (Grants Nos. 10904150 and 11274313), the Anhui Provincial Natural Science Foundation (Grant No. 1208085MA06), and the Joint Funds of the National Natural Science Foundation of China and the Chinese Academy of Sciences' Large-Scale Scientific Facility (Grants Nos. U1232138 and U1232210). Y. P. Sun acknowledges support by the National Key Basic Research (Grant No. 2011CBA00111).

References

1 H. Schmid, 1994, Ferroelectrics **162**, 317.
2 W. Eerenstein, N. D. Mathur, and J. F. Scott, 2006, Nature **442**, 759.
3 S. W. Cheong and M. Mostovoy, 2007, Nature Mater. **6**, 13.
4 R. Ramesh and N. A. Spaldin, 2007, Nature Mater. **6**, 21.
5 X. D. Qi, J. Dho, R. Tomov, M. G. Blamire and J. L. MacManus-Driscoll, 2005, Appl. Phys. Lett.**86**, 062903.
6 W. Eerenstein, F. D. Morrison, J. Dho, M. G. Blamire, J. F. Scott, N. D.Mathur, 2005, Science **307**, 1203.
7 D. Lebeugle, D. Colson, A. Forget, M. Viret, A. M. Bataille, and A. Gukasov, 2008, Phys. Rev. Lett. **100**, 227602.

8 H. Naganuma, J. Miura, and S. Okamura, 2008, Appl. Phys. Lett. **93**, 052901.

9 C. Wang, M. Takahashi, H. Fujino, X. Zhao, E. Kume, T. Horiuchi, and S. Sakai, 2006, J. Appl. Phys. **99**, 054104.

10 Y. Hiruma, R. Aoyagi, H. Nagata, and T. Takenaka, 2005, Jpn. J. Appl. Phys. **44**, 5040.

11 Z. F. Li, C. L. Wang, W. L. Zhong, J. C. Li, and M. L. Zhao, 2003, J. Appl. Phys. **94**, 2548.

12 J. Yang, J. Hou, C. Wang, M. Zhu, and H. Yan, 2007, Appl. Phys. Lett. **91**, 023118.

13 J. Wang, J. B. Neaton, H. Zheng, V. Nagarajan, S. B. Ogale, B. Liu, D. Vieland, V. Vaithyanathan, D. G. Schlom, U. V. Waghmare, N. A. Spaldin,K. M. Rabe, M. Wuttig, and R. Ramesh, 2003, Science **299**, 1719.

14 M. I. Morozov, M. A. Einarsrud, and T. Grande, 2012, Appl. Phys. Lett. **101**, 252904.

15 M. I. Morozov, M. A. Einarsrud, T. Grande, and D. Damjanovic, 2012, Ferroelectrics **439**, 88.

16 H. Matsuo, Y. Noguchi, M. Miyayama, M. Suzuki, A. Watanabe, S. Sasabe, T. Ozaki, S. Mori, and T. Kamiyama, 2010, Appl. Phys. Lett. **108**, 104103.

17 C. R. Zhou, X.Y. Liu,W. Z. Li, C. L. Yuan, 2009, J. Alloys Comp. **478**, 381.

18 G. Catalan and J. F. Scott, 2009, Adv. Mater. **21**, 2463.

19 D. A. Sanchez, N. Ortega, A. Kumar, R. Roque-Malherbe, R. Polanco, J. F. Scott, and R. S. Katiyar, 2011, AIP Adv. **1**, 042169.

20 R. Nechache, C. Harnagea, A. Pignolet, F. Normandin, T. Veres, L. P. Carignan, and D. Menard, 2006, Appl. Phys. Lett. **89**, 102902.

21 T. Kanai, S. I. Ohkoshi, A. Nakajima, T. Watanabe, K. Hashimoto, 2001, Adv. Mater. **13**, 487.

22 M. M. Kumar, S. Srinath, G. S. Kumar, S. V. Suryanarayana, 1998, J. Magn. Magn. Mater. **188**, 203.

23 E. V. Ramanaa, A. Mahajanb, M. P. F. Grac, A. Srinivasc, M. A. Valente, 2014, J. Eur. Ceram. Soc. **34**, 4201.

24 E. A. Patterson, and D. P. Cann, 2012, Appl. Phys. Lett. **101**, 042905.

25 A. Singh, and R. Chatterjee, 2011, J. Appl. Phys. **109**, 024105.

26 J. F. Scott and C. A. P. Araujo, 1989, Science **246**, 1400.

27 C. A. Randall, N. Kim, J. Kucera, W. Cao, and T. R. Shrout, 1998, J. Am. Ceram. Soc. **81**, 677.

28 D. P. Song, X. Z. Zuo, B Yuan, X. W. Tang, W. H. Song, J. Yang, X. B. Zhu, and Y. P. Sun, 2015, Cryst. Eng. Comm. **17**, 1609.

29 J. X. Zhang, Q. He, M. Trassin, W. Luo, D. Yi, M. D. Rossell, P. Yu, L. You, C. H. Wang, C. Y. Kuo, J. T. Heron, Z. Hu, R. J. Zeches, H. J. Lin, A. Tanaka, C. T. Chen, L. H. Tjeng, Y. H. Chu and R. Ramesh, 2011, Phys. Rev. Lett. **107**, 147602.

30 R. E. Cohen, Nature, 1992, **358**, 136.

31 H. Sun, X. M. Lu, T. T. Xu, J. Su, Y. M. Jin, C. C. Ju, F. Z. Huang, and J. S. Song, J. Appl. Phys., 2012, **111**, 124116.